THE JOURNAL OF PHYSICAL CHEMISTRY B

Subscriber access provided by NATIONAL TAIWAN UNIV

Article

Electrophoresis of a Spherical Dispersion of Polyelectrolytes in a Salt-Free Solution

Chia-Ping Chiang, Eric Lee, Yen-Ying He, and Jyh-Ping Hsu

J. Phys. Chem. B, **2006**, 110 (3), 1490-1498 • DOI: 10.1021/jp054969r

Downloaded from http://pubs.acs.org on November 21, 2008

More About This Article

Additional resources and features associated with this article are available within the HTML version:

- Supporting Information
- Links to the 8 articles that cite this article, as of the time of this article download
- Access to high resolution figures
- Links to articles and content related to this article
- Copyright permission to reproduce figures and/or text from this article

View the Full Text HTML

ACS Publications
High quality. High impact.

The Journal of Physical Chemistry B is published by the American Chemical Society.
1155 Sixteenth Street N.W., Washington, DC 20036

Electrophoresis of a Spherical Dispersion of Polyelectrolytes in a Salt-Free Solution

Chia-Ping Chiang, Eric Lee, Yen-Ying He, and Jyh-Ping Hsu*

Department of Chemical Engineering, National Taiwan University, Taipei, Taiwan 10617

Received: September 1, 2005; In Final Form: November 6, 2005

The electrophoretic behavior of a spherical dispersion of polyelectrolytes of arbitrary concentration is analyzed theoretically under a salt-free condition, that is, the liquid phase contains only counterions which come from the dissociation of the functional groups of polyelectrolytes. We show that, in general, the surface potential of a polyelectrolyte increases nonlinearly with its surface charge. A linear relation exists between them, however, when the latter is sufficiently small; and the more dilute the concentration of polyelectrolytes, the broader the range in which they are linearly correlated. If the amount of surface charge is sufficiently large, counterion condensation occurs, and the rate of increase of surface potential as the amount of surface charge increases declined. Also, it leads to an inverse in the perturbed potential near the surface of a polyelectrolyte, and its mobility decreases accordingly. For a fixed amount of surface charge, the lower the concentration of polyelectrolytes and/or the lower the valence of counterions, the higher the surface potential. The qualitative behavior of the mobility of a polyelectrolyte as the amount of its surface charge varies is similar to that of its surface charge.

1. Introduction

Electrophoresis, the migration of charged entities of colloidal size as a response to an applied electric field, has various applications in practice, including estimation of the charged conditions of an entity, as a separation tool, and as a displayer such as e-paper, to name a few. Under the conditions of infinitely thin double layer and low surface potential, Smoluchowski[1] was able to show that the electrophoretic velocity of an isolated particle in an infinite electrolyte medium per unit of applied electric field is proportional to its surface potential. A similar analytical expression was derived by Huckel[2] for the case of an infinitely thick double layer. Many attempts were made in subsequent studies to extend these analyses to conditions that are more plausible and/or realistic. Unfortunately, because of its complicated nature, solving a general electrophoresis problem is still challenging nowadays even if a numerical approach is adopted.

Salt-free dispersions comprise a special class of dispersed system where the ionic species in the dispersion medium come solely from the dissociation of the functional groups of the dispersed phase. A typical example in practice includes an aqueous dispersion of polyelectrolyte, a macromolecule containing dissociable functional groups. The dissociation of these functional groups yields a poly-ion backbone and counterions in the liquid phase. The specific electrical interaction between poly-ion backbone and counterions leads to behaviors that are unique to such a dispersed system. A polyelectrolyte such as polyacid, polybase, or polyampholyte can come from natural sources such as proteins and nucleic acids. DNA, the carrier of the genetic code, is also a polyelectrolye. Artificial polyelectrolytes are also ubiquitous in real life. The water-absorbing materials used in diapers and fixatures, for example, belong to this category. Other areas in which synthetic polyelectrolytes can play a key role include reverse osmosis, ion exchange, frictional drag reduction, and oil recovery.[3] A salt-free dispersion usually comprises a dispersion medium which is electrolyte-free or the degree of dissociation of the electrolyte it contains is negligible in comparison to those dissociated from the dispersed phase. An aqueous polyelectrolyte dispersion can be treated as a salt-free dispersion when the concentrations of hydrogen ions and hydroxide ions are much lower than the concentration of the counterions dissociated from polyelectrolyte.

The electrokinetic phenomenon of a salt-free dispersion was investigated first by Imai and Oosawa[4] and Oosawa[5] under the conditions of low particle concentration. The relation between the surface charge density and the surface potential of a spherical dispersion was discussed, and it was concluded that there exists a critical value for the surface charge density or the surface potential. The so-called counterion condensation occurs when this critical value is reached. On the basis of the theory of Imai and Oosawa,[4] Ohshima[6] was able to derive an analytical expression relating the surface charge density and the surface potential for spherical particles. The electrophoretic mobility of a spherical dispersion was also derived under the conditions of weak applied electric field,[7] and the approximate analytical result obtained was justified by solving two transformed electrokinetic equations by an iteration method.[8] It was found that, if the amount of fixed charge carried by a particle is small, its mobility increases linearly with the amount of fixed charge. On the other hand, if the amount of fixed charge is large, because of counterion condensation, the mobility becomes independent of the amount of fixed charge. The analysis of Ohshima[6−8] was limited to a medium concentration of particles, and the rationale behind the results observed was not discussed in detail. Adopting a molecular simulation approach, Lobaskin et al.[9] investigated the electrophoresis of colloidal particles in a salt-free medium. If the amount of fixed charge carried by a particle is small, they arrived at the same result as that of Ohshima.[7,8] However, if it is large, they found that, because over half the amount of counterions in the liquid phase move in the same direction as the particles, the mobility decreased with an increase in the

* Tel: 886-2-23637448. Fax: 886-2-23623040. E-mail: jphsu@ntu.edu.tw.

10.1021/jp054969r CCC: $33.50 © 2006 American Chemical Society
Published on Web 01/04/2006

amount of fixed charge. Colby et al.[10] applied the scaling model of De Gennes[11] to construct an alternating current conductivity model and evaluated the degree of counterion condensation through experiment. On the basis of the counterion condensation theory of Manning,[12] Bordi et al.[13] studied the conductivity of a polyelectrolyte in a low-frequency electric field. The influences of the concentration of the polyelectrolyte, its molecular weight, and the temperature on the conductivity were investigated, and the results obtained were justified by experiment. Bordi et al.[14] showed that, if the concentration of polyelectrolytes is low, the effective surface charge correlates positively with that concentration. On the other hand, if it is high, the concentration of mobile counterions decreases with the concentration of polyelectrolyte.

In this work, the electrophoresis of a spherical dispersion of polyelectrolytes in a salt-free solution is investigated. The analysis of Ohshima[6−8] is extended to the case of arbitrary polyelectrolyte concentrations. The influences of the electric Pelect number and the valence of counterions on the electrophoretic mobility of polyelectrolytes are examined. The rationales behind the occurrence of the specific behaviors of the electrophoretic mobility before and after counterion condensation are explained in detail. The unit cell model of Kuwabara[15] is adopted to simulate the spherical dispersion, and the governing equations and associated boundary conditions are solved by a pseudo-spectral method[16] based on Chebyshev polynomials. The influences of the key parameters of the system under consideration on the electrophoresis behavior of polyelectrolytes are discussed.

2. Theory

Referring to Figure 1a, we consider a dispersed system where the dispersed phase contains monodispersed spherical polyelectrolytes of radius a, and the dispersion medium is salt-free, containing only counterions dissociated from the functional groups of polyelectrolytes. A uniform electric field **E** is applied in the Z-direction, and **U** is the electrophoretic velocity of polyelectrolytes. The dispersion system is simulated by Kuwabara's unit cell model shown in Figure 1b where a representative cell comprises a representative polyelectrolyte and a concentric spherical shell of radius b. The spherical coordinate (r, θ, φ) is adopted with its origin located at the center of the polyelectrolyte. The volumetric fraction of polyelectrolytes can be estimated by $H^3 = (a/b)^3$.

2.1. Governing Equations. The spatial variation of the electrical potential ϕ can be described by the Poisson equation as[17]

$$\nabla^2\phi = -\frac{\rho}{\epsilon} \tag{1}$$

where ∇^2 is the Laplace operator, ϵ is the permittivity of the dispersion medium, and $\rho = -zen$ is the space charge density, with $-z$, n, and e being, respectively, the valence and the number density of counterions and the elementary charge.

At the steady state, the conservation of the amount of counterions leads to[17]

$$\nabla^2 n - \frac{ze}{kT}(\nabla n\cdot\nabla\phi + n\nabla^2\phi) - \frac{1}{D}(\mathbf{v}\cdot\nabla n) = 0 \tag{2}$$

where ∇ is the del operator, D is the diffusivity of counterions, **v** is the velocity of the dispersion medium, and k and T are the Boltzmann constant and the absolute temperature, respectively.

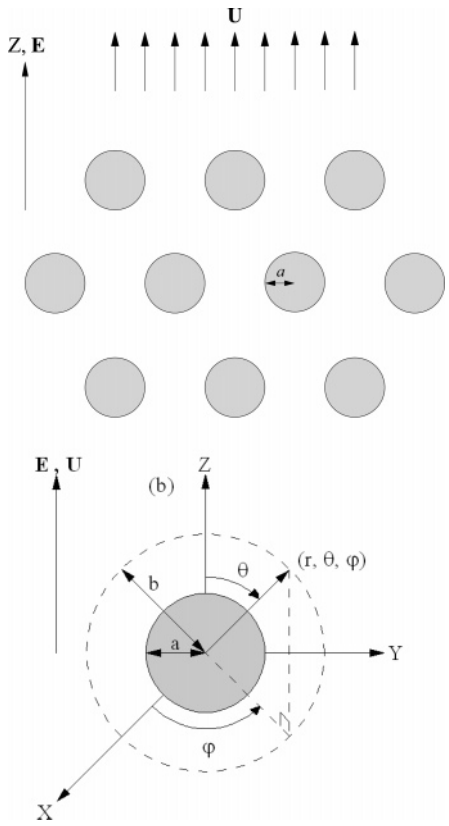

Figure 1. (a) Problem considered where an electric field **E** in the Z-direction is applied to a dispersion of spherical polyelectrolytes of radius a, and **U** is the electrophoretic velocity. (b) Kuwabara's unit cell model where the dispersion in (a) is simulated by a representative cell comprising a polyelectrolyte and a concentric spherical liquid shell of radius b. The spherical coordinates (r, θ, φ) are adopted with its origin located at the center of the polyelectrolyte.

We assume that the liquid phase is an incompressible Newtonian fluid having constant physical properties. For electrophoresis, the flow field is in the creeping flow regime, that is, the convective term in the equation of motion can be neglected, and it can be shown that in terms of the stream function ψ this equation becomes[17]

$$\mu E^4\psi = \left(\frac{\partial\phi}{\partial\theta}\frac{\partial\rho}{\partial r} - \frac{\partial\phi}{\partial r}\frac{\partial\rho}{\partial\theta}\right)\sin\theta \tag{3}$$

where

$$E^4 = E^2\cdot E^2 \text{ with } E^2 = \left[\frac{\partial}{\partial r^2} + \frac{\sin\theta}{r^2}\frac{\partial}{\partial\theta}\left(\frac{1}{\sin\theta}\frac{\partial}{\partial\theta}\right)\right]$$

and μ is the viscosity of dispersion medium. Note that, since the continuity equation is satisfied automatically by ψ, the flow field is defined solely by eq 3. Also, in terms of ψ, the r- and θ-components of the velocity **v**, v_r and v_θ, can be expressed, respectively, by

$$v_r = -\frac{1}{r^2\sin\theta}\frac{\partial\psi}{\partial\theta} \text{ and } v_\theta = \frac{1}{r\sin\theta}\frac{\partial\psi}{\partial r}$$

Suppose that the applied electric field is weak relative to that established by a polyelectrolyte. For an easier mathematical treatment,[17,18] ϕ is partitioned into the equilibrium potential ϕ_e, or the potential in the absence of **E**, and a perturbed electrical potential $\delta\phi$, which arises from the presence of **E**, that is, $\phi =$

$\phi_e + \delta\phi$. It can be shown that the governing equations for the equilibrium potential ϕ_e and the perturbed electrical potential $\delta\phi$ are, respectively,[17]

$$\nabla^2\phi_e = \frac{zen_0}{\epsilon}\exp\left(\frac{ze}{kT}\phi_e\right) \tag{4}$$

and

$$\nabla^2\delta\phi = \frac{zen_0}{\epsilon}\left[\exp\left(\frac{ze}{kT}\phi\right) - \exp\left(\frac{ze}{kT}\phi_e\right)\right] \tag{5}$$

where n_0 is the bulk concentration of counterions. A perturbed function g is introduced below to take account of the deformation of the ionic cloud surrounding a polyelectrolyte arising from its movement[18]

$$n = n_0\exp\left[\frac{ze(\phi_e + \delta\phi + g)}{kT}\right] \tag{6}$$

Applying this expression yields

$$\nabla^2\delta\phi = \frac{zen_0}{\epsilon}\left\{\exp\left[\frac{ze}{kT}(\phi_e + \delta\phi + g)\right] - \exp\left(\frac{ze}{kT}\phi_e\right)\right\} \tag{7}$$

$$\mu E^4\psi = \epsilon\kappa^2\exp\left(\frac{ze}{kT}\phi_e\right)\frac{d\phi_e}{dr}\frac{\partial g}{\partial\theta}\sin\theta \tag{8}$$

In terms of scaled symbols, eqs 4, 7, and 8 can be rewritten as

$$\nabla^{*2}\phi_e^* = \frac{(\kappa a)^2}{z}\exp(z\phi_e^*) \tag{9}$$

$$\nabla^{*2}\delta\phi^* = \frac{(\kappa a)^2}{z}\{\exp[z(\phi_e^* + \delta\phi^* + g^*)] - \exp(z\phi_e^*)\} \tag{10}$$

$$E^{*4}\psi^* = (\kappa a)^2\exp(z\phi_e^*)\frac{d\phi_e^*}{dr^*}\frac{\partial g^*}{\partial\theta}\sin\theta \tag{11}$$

where $\nabla^{*2} = a^2\nabla^2$, $\phi_e^* = \phi_e/(kT/e)$, $\delta\phi^* = \delta\phi/(kT/e)$, $g^* = g/(kT/e)$, $E^{*2} = a^2E^2$, $E^{*4} = E^{*2}\cdot E^{*2}$, and $\kappa = [(ze)^2n_0/\epsilon kT]^{1/2}$, which is the Debye−Huckel parameter, $\psi^* = \psi/a^2U_E$, and $U_E = \epsilon(kT/e)^2/\mu a$, which is a reference velocity equivalent to the electrophoretic velocity of an isolated particle predicted by the Smoluchowski's theory when an electric field (ζ_a/a) is applied where ζ_a is the ζ potential of that particle.

The governing equation for the perturbed function g can be derived from eqs 2 and 6, and it can be shown that[17]

$$\nabla^2 g + \frac{ze}{kT}\nabla g\cdot(\nabla\phi_e + \nabla\delta\phi + \nabla g) - \frac{1}{D}\mathbf{v}\cdot(\nabla\phi_e + \nabla\delta\phi + \nabla g) = 0 \tag{12}$$

In scaled form, we have

$$\nabla^{*2}g^* + z\nabla^* g^*\cdot\nabla^*(\phi_e^* + \delta\phi^* + g^*) = \mathrm{Pe}\mathbf{v}^*\cdot\nabla^*(\phi_e^* + \delta\phi^* + g^*) \tag{13}$$

where $\mathrm{Pe} = \epsilon(e/kT)^2/\mu D$ is the electric Pelect number of counterions, and $\mathbf{v}^* = \mathbf{v}/U_E$ is the scaled velocity of the dispersion medium.

2.2. Boundary Conditions. The following boundary conditions are assumed for the equilibrium potential ϕ_e:

$$\frac{d\phi_e}{dr} = -\frac{\sigma}{\epsilon} \quad r = a \tag{14}$$

$$\frac{d\phi_e}{dr} = 0 \quad r = b \tag{15}$$

where σ represents the surface charge density. Here, we assume that the surface charge density remains constant and the unit cell as a whole is electrically neutral, which implies that there is net current across the cell boundary. The total amount of surface charge on a polyelectrolyte can be expressed as

$$Q_s = 4\pi a^2\sigma = \frac{4}{3}\pi(b^3 - a^3)zen_0 \tag{16}$$

The following boundary conditions are assumed for the perturbed electric potential $\delta\phi$:

$$\frac{\partial\delta\phi}{\partial r} = 0 \quad r = a \tag{17}$$

$$\delta\phi = -E_z b\cos\theta \quad r = b \tag{18}$$

where E_z is the Z-component of $\mathbf{E}$. The first expression is based on the fact that polyelectrolytes are nonconductive, and the second expression was proposed by Shilov et al.[19] and arises from the nature of Kuwabara's unit cell model, that is, since cell boundary corresponds to system boundary, the electric field over there is that contributed by the applied electric field only.

Since the ionic concentration should reach its bulk value on the cell surface ($r = b$), and the surface of polyelectrolyte is ion-impenetrable, we have

$$\frac{\partial g}{\partial r} = 0 \quad r = a \tag{19}$$

$$g = -\delta\phi \quad r = b \tag{20}$$

For convenience, we let the representative polyelectrolyte be fixed in the flow field, and the fluid on the cell surface moves in the Z-direction with a relative velocity of $-\mathbf{U}$. Also, the vorticity on the cell surface vanishes. In terms of the stream function ψ, these lead to the following boundary conditions for the flow field:

$$\psi = 0 \quad r = a \tag{21}$$

$$\frac{\partial\psi}{\partial r} = 0 \quad r = a \tag{22}$$

$$\psi = \frac{1}{2}r^2U\sin^2\theta \quad r = b \tag{23}$$

$$\frac{\partial^2\psi}{\partial r^2} + \frac{\sin\theta}{r^2}\frac{\partial}{\partial\theta}\left(\frac{1}{\sin\theta}\frac{\partial\psi}{\partial\theta}\right) = 0 \quad r = b \tag{24}$$

Also, the symmetric nature of the present problem requires that

$$\frac{\partial\phi_e}{\partial\theta} = \frac{\partial\delta\phi}{\partial\theta} = \frac{\partial g}{\partial\theta} = \psi = \frac{\partial\psi}{\partial\theta} = 0 \quad \theta = 0 \text{ or } \theta = \pi \tag{25}$$

Equations 14−25 can be expressed in terms of scaled symbols as follows:

$$\frac{d\phi_e^*}{dr^*} = -\frac{(\kappa a)^2}{3z}\left[\left(\frac{1}{H}\right)^3 - 1\right] \quad r^* = 1 \tag{26}$$

$$\frac{d\phi_e^*}{dr^*} = 0 \quad r^* = \frac{b}{a} = \frac{1}{H} \tag{27}$$

$$Q_s^* = \frac{(\kappa a)^2}{3z}\left[\left(\frac{1}{H}\right)^3 - 1\right] \tag{28}$$

$$\frac{\partial \delta\phi^*}{\partial r^*} = 0 \quad r^* = 1 \tag{29}$$

$$\delta\phi^* = -E_z^* \frac{b}{a}\cos\theta \quad r^* = \frac{b}{a} = \frac{1}{H} \tag{30}$$

$$\frac{\partial g^*}{\partial r^*} = 0 \quad r^* = 1 \tag{31}$$

$$g^* = -\delta\phi^* \quad r^* = \frac{b}{a} = \frac{1}{H} \tag{32}$$

$$\psi^* = 0 \quad r^* = 1 \tag{33}$$

$$\frac{\partial \psi^*}{\partial r^*} = 0 \quad r^* = 1 \tag{34}$$

$$\psi^* = \frac{1}{2} r^{*2} U^* \sin^2\theta \quad r^* = \frac{b}{a} = \frac{1}{H} \tag{35}$$

$$\frac{\partial^2 \psi^*}{\partial r^{*2}} + \frac{\sin\theta}{r^{*2}} \frac{\partial}{\partial\theta}\left(\frac{1}{\sin\theta}\frac{\partial \psi^*}{\partial\theta}\right) = 0 \quad r^* = \frac{b}{a} = \frac{1}{H} \tag{36}$$

$$\frac{\partial \phi_e^*}{\partial\theta} = \frac{\partial \delta\phi^*}{\partial\theta} = \frac{\partial g^*}{\partial\theta} = \psi^* = \frac{\partial \psi^*}{\partial\theta} = 0 \quad \theta = 0 \text{ or } \theta = \pi \tag{37}$$

In these expressions, $Q_s^* = Q_s(e/kT)/4\pi\epsilon a$, $E_z^* = E_z(e/kT)/a$, and $U^* = U/U_E$.

By applying the method of separation of variables, each of the scaled functions $\delta\phi^*$, g^*, and ψ^* is expressed as a product of a radial function and an angular function, and the solutions to eqs 9, 10, 11, and 13 subject to eqs 26−37 take the forms

$$\delta\phi^* = \delta\Phi^*(r^*)\cos\theta \tag{38}$$

$$g^* = \mathrm{G}^*(r^*)\cos\theta \tag{39}$$

$$\psi^* = \Psi^*(r^*)\sin^2\theta \tag{40}$$

where $\delta\Phi^*(r^*)$, $G^*(r^*)$, and $\Psi^*(r^*)$ are, respectively, the radial parts of $\delta\phi^*$, g^*, and ψ^*. On the basis of these expressions, eqs 9, 10, 11, 13, and 26−37 lead to

$$L_r^{*2}\phi_e^* = \frac{(\kappa a)^2}{z}\exp(z\phi_e^*) \tag{41}$$

$$L^{*2}\delta\Phi^* - (\kappa a)^2\exp(z\phi_e^*)\delta\Phi^* = (\kappa a)^2\exp(z\phi_e^*)G^* \tag{42}$$

$$\frac{\mathrm{d}\delta\Phi^*}{\mathrm{d}r^*} = 0 \quad r^* = 1 \tag{43}$$

$$\delta\Phi^* = -E_z^* \frac{b}{a} \quad r^* = \frac{b}{a} = \frac{1}{H} \tag{44}$$

$$L^{*2}G^* = -z\frac{\mathrm{d}\phi_e^*}{\mathrm{d}r^*}\frac{\mathrm{d}G^*}{\mathrm{d}r^*} - 2\frac{\mathrm{Pe}}{r^{*2}}\frac{\mathrm{d}\phi_e^*}{\mathrm{d}r^*}\Psi^* \tag{45}$$

$$\frac{\mathrm{dG}^*}{\mathrm{d}r^*} = 0 \quad r^* = 1 \tag{46}$$

$$G^* = -\delta\Phi^* \quad r^* = \frac{b}{a} = \frac{1}{H} \tag{47}$$

$$D^{*4}\Psi^* = -(\kappa a)^2\exp(z\phi_e^*)\frac{\mathrm{d}\phi_e^*}{\mathrm{d}r^*}G^* \tag{48}$$

$$\Psi^* = 0 \quad r^* = 1 \tag{49}$$

$$\frac{\mathrm{d}\Psi^*}{\mathrm{d}r^*} = 0 \quad r^* = 1 \tag{50}$$

$$\Psi^* = \frac{1}{2} r^{*2} U^* \quad r^* = \frac{b}{a} = \frac{1}{H} \tag{51}$$

$$\frac{\mathrm{d}^2\Psi^*}{\mathrm{d}r^{*2}} - \frac{2\Psi^*}{r^{*2}} = 0 \quad r^* = \frac{b}{a} = \frac{1}{H} \tag{52}$$

The scaled one-dimensional operators used in these expressions are defined by

$$L_r^{*2} = \frac{\mathrm{d}^2}{\mathrm{d}r^{*2}} + \frac{2}{r^*}\frac{\mathrm{d}}{\mathrm{d}r^*},\ L^{*2} = \frac{\mathrm{d}^2}{\mathrm{d}r^{*2}} + \frac{2}{r^*}\frac{\mathrm{d}}{\mathrm{d}r^*} - \frac{2}{r^{*2}},$$
$$D^{*2} = \frac{\mathrm{d}^2}{\mathrm{d}r^{*2}} - \frac{2}{r^{*2}},\ \text{and}\ D^{*4} = D^{*2}D^{*2}$$

The electrophoretic mobility of a polyelectrolyte can be evaluated on the basis of the fact that the sum of the forces acting on it vanishes at steady state. For the present problem, only the Z-component of those forces, which include the electrical force, F_{Ez}, and the hydrodynamic force, F_{Hz}, need to be considered. We have

$$F_{Ez} + F_{Hz} = 0 \tag{53}$$

or in terms of scaled symbols as

$$F_{Ez}^* + F_{Hz}^* = 0 \tag{54}$$

where $F_{Ez}^* = F_{Ez}/\epsilon(kT/e)^2$, $F_{Hz}^* = F_{Hz}/\epsilon(kT/e)^2$. The Z-component of the electrical force acting on a polyelectrolyte can be evaluated by

$$F_{Ez} = (\mathbf{F}_E\cdot\delta_z)_S = \int_S [\sigma(\mathbf{E})_S\cdot\delta_z]_S\,\mathrm{d}A \tag{55}$$

where the subscript S denotes the surface of a polyelectrolyte, $\mathbf{F}_E$ is the electrical force, $\boldsymbol{\delta}_z$ is the unit vector in the Z-direction, and $(\mathbf{E})_S$ is the applied electric field on S. It can be shown that[17]

$$F_{Ez} = -2\pi\epsilon\left(\frac{kT}{e}\right)^2\frac{\mathrm{d}\phi_e^*}{\mathrm{d}r^*}\bigg|_{r^*=1}\int_0^\pi\left(\frac{\partial\delta\phi^*}{\partial\theta}\right)_{r^*=1}\sin^2\theta\,\mathrm{d}\theta =$$
$$\frac{8}{3}\pi\epsilon\left(\frac{kT}{e}\right)^2\frac{\mathrm{d}\phi_e^*}{\mathrm{d}r^*}\delta\Phi^*\bigg|_{r^*=1} \tag{56}$$

The Z-component of the hydrodynamic force acting on a polyelectrolyte includes the drag on a charge-free polyelectrolyte, and that arises from the presence of charge on its surface. The former can be evaluated by the method of Happel and Brenner.[20] It can be shown that[17]

$$F_{Hz} = \pi\epsilon\left(\frac{kT}{e}\right)^2 \int_0^\pi \left[r^{*4} \sin\theta \frac{\partial}{\partial r^*}\left(\frac{E^{*2}\psi^*}{r^{*2}}\right)\right]\Big|_{r^*=1} d\theta + \pi\epsilon\left(\frac{kT}{e}\right)^2 \frac{(\kappa a)^2}{z} \int_0^\pi \left\{r^{*2} \sin^2\theta \exp(\alpha\phi_e^*) \times [1 + \alpha(\delta\Phi^* + g^*)] \frac{\partial\delta\phi^*}{\partial\theta}\right\}\Big|_{r^*=1} d\theta$$

$$= \frac{4}{3}\pi\epsilon\left(\frac{kT}{e}\right)^2 \left|\left[r^{*2}\frac{d(D^{*2}\Psi^*)}{dr^*} - r^{*2}\frac{(\kappa a)^2}{z} \times \exp(z\phi_e^*)\delta\Phi^*\right]\right|_{r^*=1} - \frac{8}{3}\left|\pi\epsilon\left(\frac{kT}{e}\right)^2 (r^* D^{*2}\Psi^*)\right|_{r^*=1}$$

$$= F_{HFz} + F_{HSz} \quad (57)$$

where F_{HFz} and F_{HSz} are, respectively, the viscous form drag and the viscous skin drag acting on a polyelectrolyte. In these expressions

$$F_{HFz} = \frac{4}{3}\pi\epsilon\left(\frac{kT}{e}\right)^2 \left[r^{*2}\frac{d(D^{*2}\Psi^*)}{dr^*} - r^{*2}\frac{(\kappa a)^2}{z}\exp(z\phi_e^*)\delta\Phi^*\right]\Big|_{r^*=1} \quad (58)$$

$$F_{HSz} = -\frac{8}{3}\pi\epsilon\left(\frac{kT}{e}\right)^2 (r^* D^{*2}\psi^*)\Big|_{r^*=1} \quad (59)$$

Equations 58 and 59 can be rewritten in scaled form as

$$F_{Ez}^* = \frac{8}{3}\pi\frac{d\phi_e^*}{dr^*}\delta\Phi^*\Big|_{r^*=1} \quad (60)$$

$$F_{Hz}^* = \frac{4}{3}\pi\left[r^{*2}\frac{d(D^{*2}\Psi^*)}{dr^*} - r^{*2}\frac{(\kappa a)^2}{z}\exp(z\phi_e^*)\delta\Phi^* - 2r^* D^{*2}\Psi^*\right]\Big|_{r^*=1} \quad (61)$$

$$= F_{HFz}^* + F_{HSz}^*$$

where

$$F_{HFz}^* = \frac{4}{3}\pi\left[r^{*2}\frac{d(D^{*2}\Psi^*)}{dr^*} - r^{*2}\frac{(\kappa a)^2}{z}\exp(z\phi_e^*)\delta\Phi^*\right]\Big|_{r^*=1} \quad (62)$$

and

$$F_{HSz}^* = -\frac{8}{3}\pi(r^* D^{*2}\psi^*)\Big|_{r^*=1} \quad (63)$$

are, respectively, the scaled viscous form drag and the scaled viscous skin drag acting on a polyelectrolyte.

The set of governing equations, eqs 41, 42, 45, and 48, and the associated boundary conditions are solved numerically by a pseudo-spectral method[16] based on Chebyshev polynomials. Previous experience[17] indicates that this approach is efficient and accurate for a problem of the present type.

3. Results and Discussion

Figure 2 shows the variation of the scaled surface potential, ζ_s^* ($= \phi_e^*(1) - \phi_e^*(1/H)$), as a function of the scaled total charge on a polyelectrolyte, Q_s^*, at various volumetric fractions of polyelectrolytes, H^3. This figure reveals that, in general, ζ_s^* increases with Q_s^* nonlinearly. However, if Q_s^* is sufficiently small, ζ_s^* increases with Q_s^* linearly. For example, for $H^3 = 10^{-6}$, $\zeta_s^* = Q_s^*$ for Q_s^* in the range [1, 10]. Note that the more dilute the concentration of polyelectrolytes the broader the range in which ζ_s^* is linearly dependent on Q_s^*. These behaviors were also observed by Ohshima,[6] except that his results were limited to low polyelectrolyte concentrations; counterion condensation was proposed to explain those behaviors without detailed discussions. The results shown in Figure 2 can be explained by the counterions in the liquid phase coming solely from the dissociation of the functional groups on the polyelectrolyte

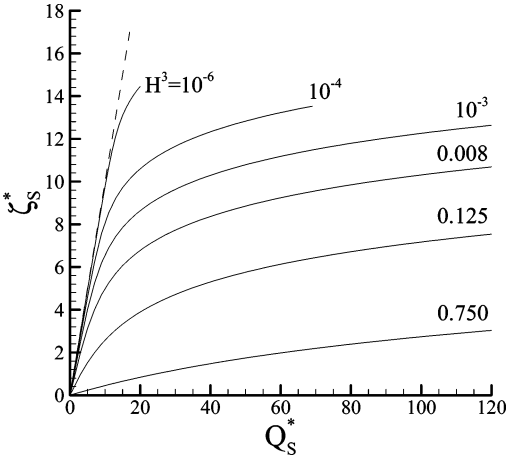

Figure 2. Variation of scaled ζ potential, ζ_s^*, as a function of Q_s^* at various values of H for the case when $z = 1$.

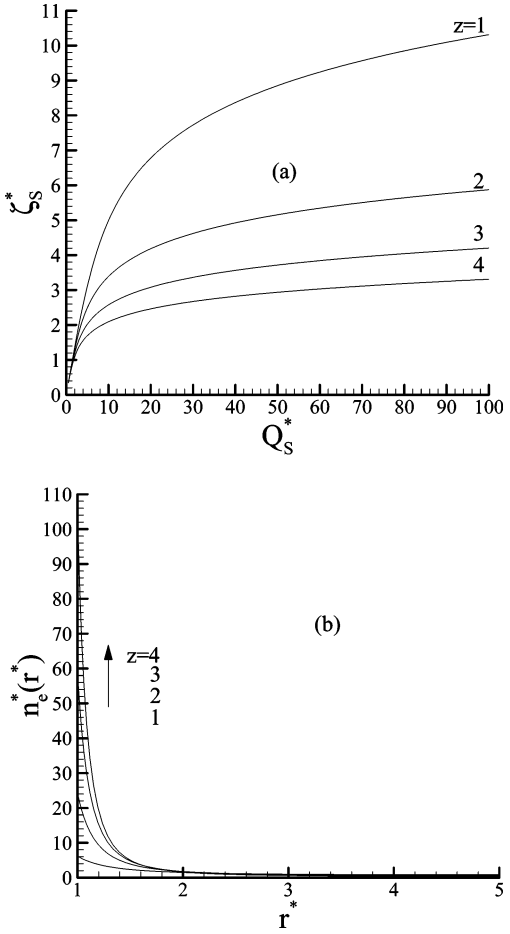

Figure 3. (a) Variation of scaled ζ potential, ζ_s^*, as a function of Q_s^* at various values of z for the case when $H^3 = 0.008$. (b) Spatial distribution of counterions at various values of z for the case when $Q_s^* = 3$ and $H^3 = 0.008$.

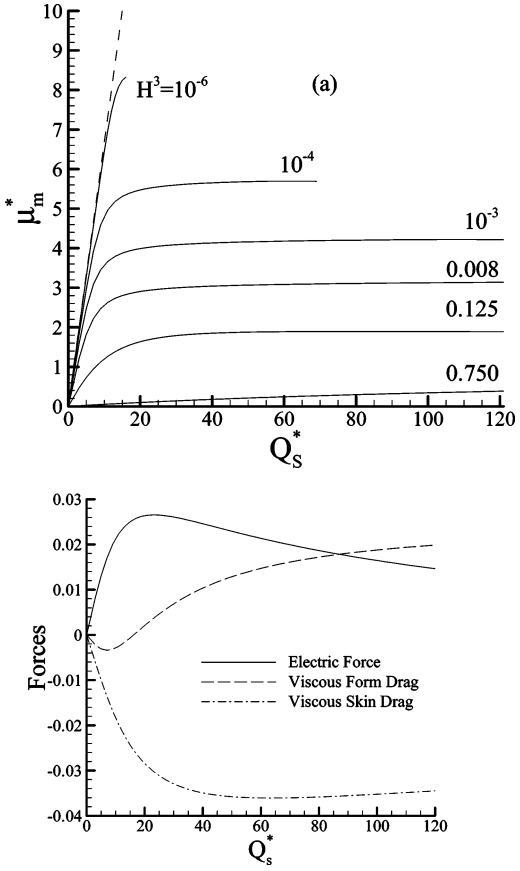

Figure 4. (a) Variation of scaled electrophoretic mobility μ_m^* as a function of Q_s^* at various values of H for the case when $z = 1$ and Pe $= 0.256$. (b) Variations of the scaled electric force, viscous form drag, and skin drag acting on a polyelectrolyte as a function of Q_s^* for the case of (a) except that $H^3 = 0.125$.

surface, and the amount is the same as that of the fixed charge on the polyelectrolyte surface. If Q_s^* is small, because the interaction between a polyelectrolyte and the counterions in the liquid phase is unimportant, its surface potential is determined mainly by the amount of surface charge. In the case when the concentration of polyelectrolytes is low, the surface potential can be estimated by that established by a polyelectrolyte carrying a total amount of surface charge Q_s, $\zeta_s = Q_s/4\pi\epsilon a$, or in terms of scaled symbols, $\zeta_s^* = Q_s^*$, which is the dashed line in Figure 2. As Q_s^* increases, the electrical interaction tends to attract the counterions in the liquid phase to the surface of a polyelectrolyte, and the larger the Q_s^*, the more significant is that phenomenon, the so-called counterion condensation. In this case, the rate of increase of ζ_s^* as Q_s^* increases declined and deviates from the linear relation $\zeta_s^* = Q_s^*$. According to Figure 2, for a fixed value of Q_s^*, the smaller the value of H^3, the larger the value of ζ_s^*. This is because, if H^3 is small, there is enough space in the liquid phase for the concentration of counterions to decay to its bulk value. The absolute value of the gradient of the electrical potential near the polyelectrolyte surface is small, and so is ζ_s^*. On the other hand, if H^3 is large, the decay of the concentration of counterions is limited, and so is the absolute value of the gradient of the electrical potential near the polyelectrolyte surface and ζ_s^*.

Figure 3a indicates that, for a fixed value of Q_s^*, the higher the valence of counterions z, the smaller the value of ζ_s^*. This is expected because counterions of a higher valence are easier to attract to the surface of a polyelectrolyte than counterions of a lower valence, as is illustrated in Figure 3b. That is, the

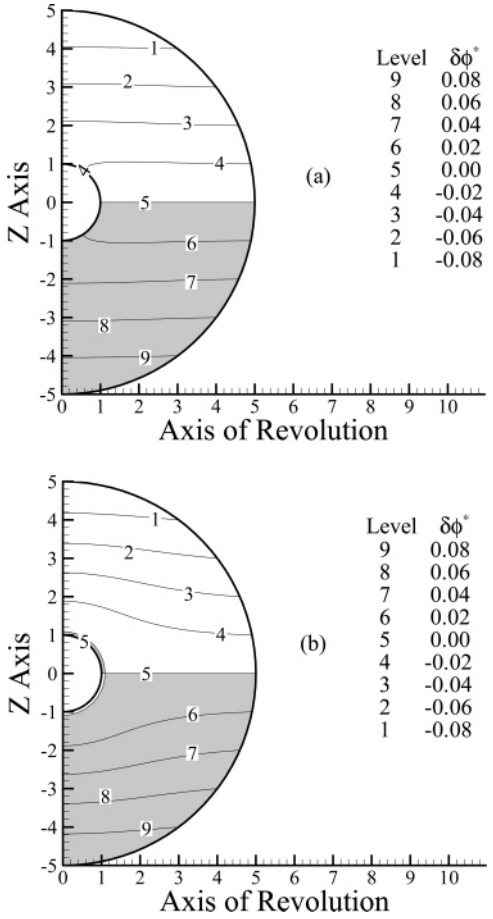

Figure 5. Contours of scaled perturbed potential $\delta\phi^*$ at different values of Q_s^* for the case when $H^3 = 0.008$, $z = 1$, and Pe $= 0.256$. The region where $\delta\phi^* > 0$ is shaded. (a) $Q_s^* = 5$; (b) $Q_s^* = 40$.

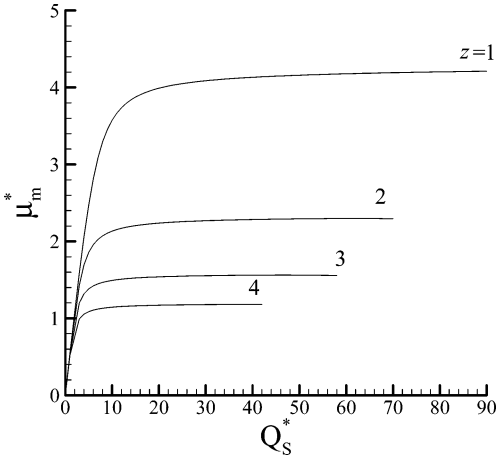

Figure 6. Variation of scaled electrophoretic mobility μ_m^* as a function of Q_s^* at various valences of counterions $-z$ for the case when $H^3 = 10^{-3}$ and Pe $= 0.256$.

phenomenon of counterion condensation is more significant for counterions of a higher valence than that of a lower valence.

The variations of the scaled electrophoretic mobility μ_m^* as a function of Q_s^* at various values of H are shown in Figure 4a, and typical variations in the scaled electric force F_{Ez}^*, scaled viscous form drag F_{HFz}^*, and scaled skin drag F_{HSz}^* as a function of Q_s^* are presented in Figure 4b. The qualitative behavior of μ_m^* observed in Figure 4a is similar to that of ζ_s^* shown in Figure 2. The dashed line in Figure 4a is $\mu_m^* = 2Q_s^*/3$, the Henry's formula, which is expected, since as discussed previ-

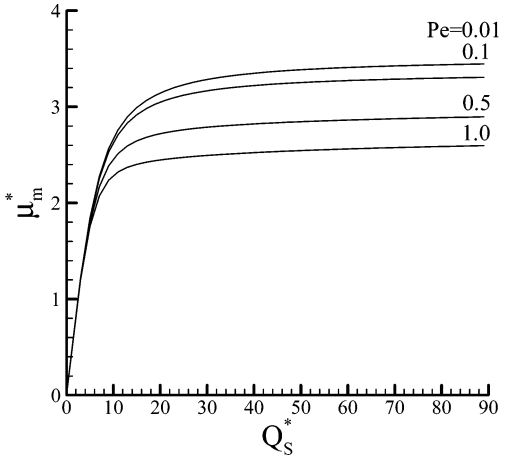

Figure 7. Variation of scaled electrophoretic mobility μ_m^* as a function of Q_s^* at various values of Pe for the case when $H^3 = 0.008$ and $z = 1$.

ously, if Q_s^* is small, the electrical interaction between the polyelectrolyte surface and the counterions is unimportant and the presence of counterions can be neglected; therefore, the mobility of a polyelectrolyte can be determined solely by its surface charge, especially when the concentration of polyelectrolytes is low. As Q_s^* increases, the electrical interaction becomes important, counterions tend to approach the polyelectrolyte surface, and as a result, the electrical force acting on a polyelectrolyte does not increase proportionally to the increase in Q_s^*. However, as shown in Figure 4b, because the skin drag on a polyelectrolyte also increases with Q_s^*, the rate of increase of μ_m^* with the increase of Q_s^* declines. For a given value of H, when Q_s^* reaches the corresponding saturation value, $Q_{s,s}^*$ ($\cong$20), a large amount of counterions are attracted to the region near a polyelectrolyte, and counterion condensation occurs. As will be discussed later, this leads to an inversion in the perturbed electrical potential near the surface of a polyelectrolyte, the electrical force acting on it decreases accordingly, as can be seen in Figure 4b, and therefore, μ_m^* should decrease with the increase in Q_s^*. However, because the reverse in $\delta\phi^*$ also leads to a decrease in form drag, μ_m^* remains roughly constant when Q_s^* exceeds $Q_{s,s}^*$. For the case when $H^3 = 0.750$, because the separation distance between polyelectrolytes is small, the hydrodynamic friction acting on a polyelectrolyte is large, and μ_m^* is small. Also, since counterion condensation is inappreciable, μ_m^* varies roughly linearly with Q_s^*. The relation between μ_m^* and Q_s^* was also discussed by Ohshima[7,8] for a medium level of polyelectrolyte concentration, and the results obtained were explained by counterion condensation only without detailed discussions, especially the variations in relevant forces.

Figure 5 shows the contours of the scaled perturbed potential $\delta\phi^*$ for two levels of Q_s^*. The region where $\delta\phi^* > 0$ is shaded in these figures. According to eq 42, $\delta\Phi^*(r^*)$, and therefore, $\delta\phi^*$, is influenced by both the applied electric field and the presence of counterions measured by G^*. Figure 5a reveals that, if Q_s^* is small, counterion condensation does not occur. In this case, the concentration of counterions in the dispersion medium is low, their presence has a negligible influence on the perturbed potential, and therefore, it is mainly determined by the applied electric field. Note that $\delta\phi^*$ is negative in the upper region of a polyelectrolyte and is positive in the lower region of the polyelectrolyte, so that $\nabla\delta\phi^*$ has the same direction as that of the applied electric field. Figure 5b shows that, if Q_s^* is large, counterion condensation occurs, leading to a high concentration

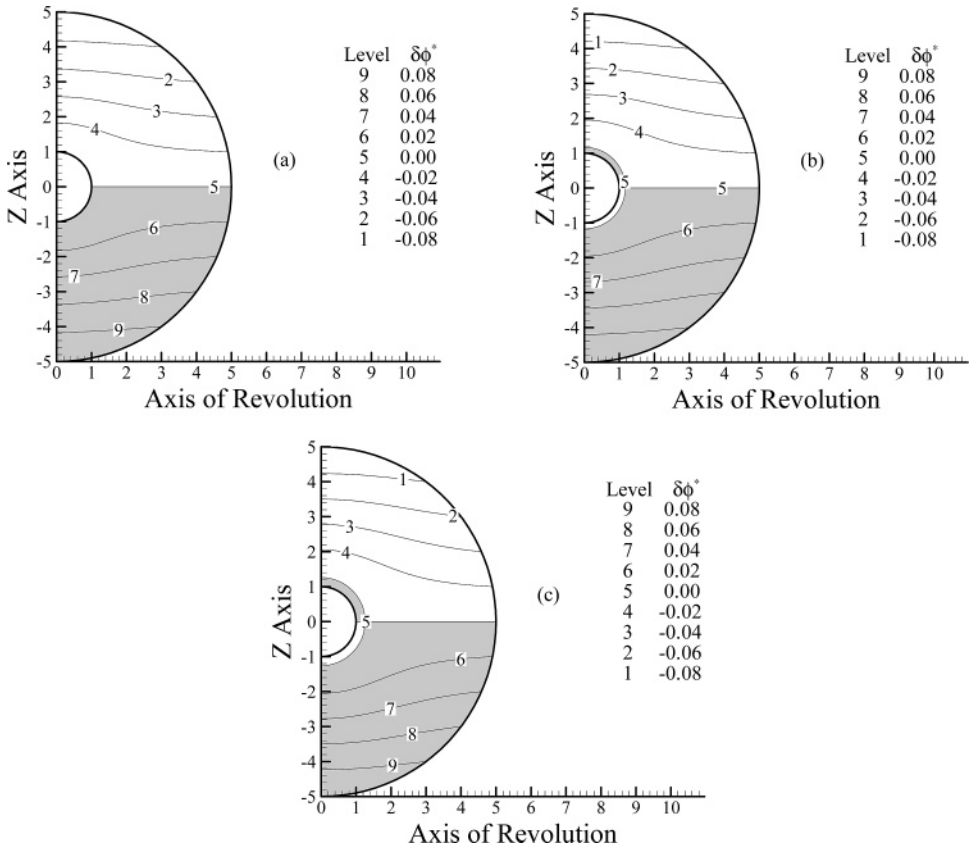

Figure 8. Contours of scaled perturbed potential $\delta\phi^*$ at various values of Pe for the case when $H^3 = 0.008$, $z = 1$, and $Q_s^* = 40$. The region where $\delta\phi^* > 0$ is shaded. (a) Pe = 0.1; (b) Pe = 0.5; (c) Pe = 1.

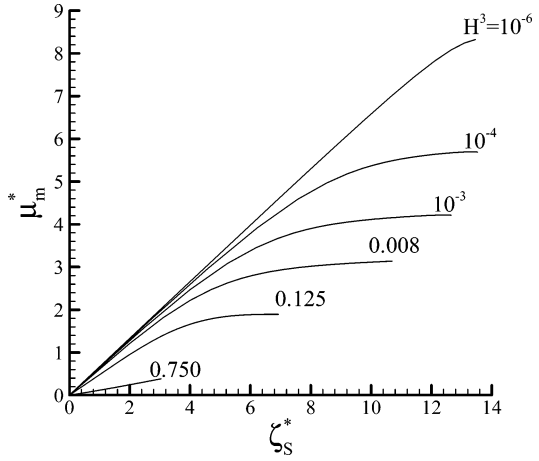

Figure 9. Variation of scaled electrophoretic mobility μ_m^* as a function of scaled ζ potential, ζ_s^*, at various values of H for the case when $z = 1$ and Pe = 0.256.

of counterions near the surface of a polyelectrolyte. As the polyelectrolyte moves in the *Z*-direction, counterions tend to migrate toward its rear part, that is, the bottom part of the polyelectrolyte in Figure 5b. This leads to an induced electric field which is in the reverse direction to that of the applied electric field, and the former is strong than the latter. The occurrence of counterion condensation also yields a low concentration of counterions in the dispersion medium, and the perturbed potential in that phase becomes determined mainly by the applied electric field.

Figure 6 shows the variation of the scaled mobility μ_m^* as a function of the scaled total amount of fixed charge Q_s^* at various valences of counterions. This figure indicated that the higher the valence of counterions the smaller the scaled mobility is. As pointed out previously, this is because, for a fixed value of Q_s^*, the higher the valence of counterions, the more easily they are attracted to the surface of a polyelectrolyte; the screening effect leads to a smaller electric force acting on the polyelectrolyte, and therefore, its mobility becomes smaller. Also, since the higher the valence of counterions, the more easily they are attracted to the surface of a polyelectrolyte, it is easier for counterion condensation to occur, which also yields a smaller mobility.

The influence of the electric Peclet number Pe on the variation of the scaled mobility μ_m^* as a function of the scaled total amount of fixed charge Q_s^* is illustrated in Figure 7. This figure suggests that, if Q_s^* is sufficiently large, the larger the Pe, the smaller the μ_m^* is. Again, this arises from the effect of counterion condensation and the establishment of an induced electric field near polyelectrolyte surface as illustrated in Figure 8 where the contours of the scaled perturbed potential $\delta\phi^*$ at various levels of Pe for the case when counterion condensation occurs ($Q_s^* = 40$). The region where $\delta\phi^* > 0$ is shaded. Pe can be interpreted as the ratio (rate of ion transfer through convection/sum of the rates of ion transfer through diffusion and through migration). If counterion condensation occurs and Pe is large, the convection term dominates, and its influence on ionic distribution is significant. In this case, the reverse of the perturbed electric field becomes serious, the electric force acting on a polyelectrolyte declines, and accordingly, its mobility becomes small. On the other hand, if Pe is small, the diffusion and migration terms dominate, the reverse of the perturbed electric field is less serious, and the mobility becomes larger.

The influence of the concentration of polyelectrolytes on the variation of μ_m^* as a function of ζ_s^* is presented in Figure 9. This figure can also be viewed as a combination of Figures 2 and 4a. In practice, if the valence of counterions, the Peclet number, and the concentration of particles are known, then Figure 9 can be used to determine ζ_s^* when μ_m^* is measured.

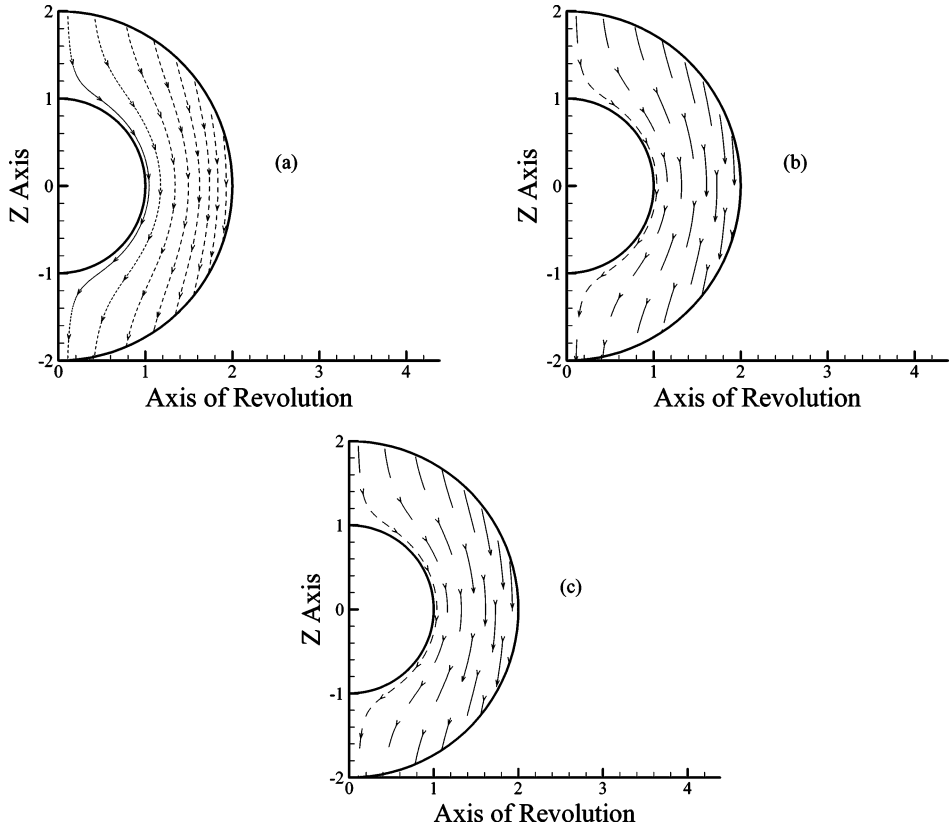

Figure 10. Variations of flow field at various values of Q_s^* for the case when $z = 1$ and $H^3 = 0.008$. (a) $Q_s^* = 1$; (b) $Q_s^* = 30$; (c) $Q_s^* = 100$.

Figure 10 shows the variations of the flow field at various values of Q_s^* for the case when $H = 0.008$. In Figure 10a, Q_s^* is small (=1). Figure 10b represents the case when counterion condensation just occurs ($Q_s^* = 30$), and Figure 10c represents the case when Q_s^* is large (=100). Here, the direction of liquid flow is expressed by the arrows, and the magnitude of liquid velocity is measured by the length of the line segment. The flow of liquid in Figure 10 is toward the *Z*-direction, because we assume that a polyelectrolyte is fixed in the flow field. Figure 10 reveals that, while the liquid velocity increases with an increase in Q_s^*, it becomes inappreciable to the variation of Q_s^* when Q_s^* exceeds $Q_{s,s}^*$.

Conclusions

In summary, the electrophoretic behavior of a spherical dispersion of polyelectrolytes is analyzed for the case when the liquid phase contains only counterions which come from the dissociation of the functional groups of a polyelectrolyte. We show that, in general, the surface potential of a polyelectrolyte increases nonlinearly with its surface charge. A linear relation exists between them, however, when the latter is sufficiently small, and the more dilute the concentration of polyelectrolytes, the broader the range in which they are linearly correlated. If the amount of surface charge is sufficiently large, counterion condensation occurs, where counterions in the dispersion medium are attracted to stay near the surface of a polyelectrolyte. In this case, the rate of increase of surface potential declines as the amount of surface charge increases. Also, it leads to an inverse in the perturbed potential near the surface of a polyelectrolyte, and its mobility decreases accordingly. For a fixed amount of surface charge, the lower the concentration of polyelectrolytes or the lower the valence of counterions, the higher the surface potential is. The qualitative behavior of the mobility of a polyelectrolyte as the amount of its surface charge varies is similar to that of its surface charge. For example, if the amount of surface charge is low, the Huckel's formula is applicable when the concentration of polyelectrolytes is low. Also, the higher the valence of counterions, the smaller the scaled mobility is. If the amount of surface charge of a polyelectrolyte is sufficiently large, its mobility decreases with the increase in the Peclet number of counterions.

Acknowledgment. This work is supported by the National Science Council of the Republic of China.

References and Notes

(1) Smoluchowski, M. *Z. Phys. Chem.* **1918**, *92*, 129.
(2) Huckel, E. *Phys. Z.* **1924**, *25*, 204.
(3) Nagvekar, M.; Tihminlioglu, F.; Danner, R. P. *Fluid Phase Equilib.* **1998**, *145*, 15.
(4) Imai, N.; Oosawa, F. *Busseiron Kenkyu* **1952**, *52*, 42.
(5) Oosawa, F. *Polyelectrolytes*; Dekker: New York, 1971.
(6) Ohshima, H. *J. Colloid Interface Sci.* **2002**, *247*, 18.
(7) Ohshima, H. *J. Colloid Interface Sci.* **2002**, *248*, 499.
(8) Ohshima, H. *J. Colloid Interface Sci.* **2003**, *262*, 294.
(9) Lobaskin, V.; Dünweg, B.; Holm, C. *J. Phys.: Condens. Matter* **2004**, *16*, S4063.
(10) Colby, R. H.; Boris, D. C.; Krause, W. E.; Tan, J. S. *J. Polym. Sci., Part B: Polym. Phys.* **1997**, *35*, 2951.
(11) De Gennes, P. G.; Pincus, P.; Velasco, R. M.; Brochard, F. *J. Phys.* **1976**, *37*, 1461.
(12) Manning, G. S. *Physica A* **1996**, *231*, 236.
(13) Bordi, F.; Cametti, C.; Notta, A.; Paradossi, G. *J. Phys. Chem.* **1999**, *103*, 5092.
(14) Bordi, F.; Colby, R. H.; Cametti, C.; De Lorenzo, L.; Gili, T. *J. Phys. Chem. B* **2002**, *10*6, 6887.
(15) Kuwabara, S. *J. Phys. Soc. Jpn.* **1959**, *14*, 527.
(16) Canuto, C.; Hussaini, M. Y.; Quarteroni, A.; Zang T. A. *Spectral Method in Fluid Dynamics*; Springer-Verlag: Berlin, 1988.
(17) Lee, E.; Chu, J. W.; Hsu, J. P. *J. Colloid Interface Sci.* **1998**, *205*, 65.
(18) O'Brien, R. W.; White, L. R. *J. Chem. Soc., Faraday Trans.* **1978**, *274*, 1607.
(19) Shilov, V. N.; Zharkikh, N. I.; Borkovskaya, Y. B. *Colloid J.* **1981**, *43*, 434.
(20) Happel, J.; Brenner, H. *Low Reynolds Number Hydrodynamics*; Martinus: Nijhoff, 1983.